Assessment of the amount of Cesium-137 released into the Pacific Ocean after the Fukushima accident and analysis of its dispersion in Japanese coastal waters

Claude Estournel, Emmanuel Bosc, Marc Bocquet, Caroline Ulses, Patrick Marsaleix, Victor Winiarek, Iolanda Osvath, Cyril Nguyen, Thomas Duhaut, Florent Lyard, et al.

Assessment of the amount of cesium-137 released into the Pacific Ocean after the Fukushima accident and analysis of its dispersion in Japanese coastal waters

C. Estournel,[1] E. Bosc,[2] M. Bocquet,[3,4] C. Ulses,[1] P. Marsaleix,[1] V. Winiarek,[3,4] I. Osvath,[2] C. Nguyen,[1,5] T. Duhaut,[1] F. Lyard,[5] H. Michaud,[1] and F. Auclair[1]

Received 30 January 2012; revised 17 September 2012; accepted 1 October 2012; published 14 November 2012.

[1] Numerical modeling was used to provide a new estimate of the amount of ^{137}Cs released directly into the ocean from the Fukushima Daiichi nuclear power plant (NPP) after the accident in March 2011 and to gain insights into the physical processes that led to its dispersion in the marine environment during the months following the accident. An inverse method was used to determine the time-dependent ^{137}Cs input responsible for the concentrations observed at the NPP's two liquid discharge outlets. The method was then validated through comparisons of the simulated concentrations with concentrations measured in seawater at different points in the neighborhood of the plant. An underestimation was noticed for stations located 30 km offshore. The resulting bias in the release inventory was estimated. Finally, the maximum ^{137}Cs activity released directly to the ocean was estimated to lie between 5.1 and 5.5 PBq (Peta Becquerel = 10^{15} Bq) but uncertainties remain on the amount of radionuclides released during the first few days after the accident. This estimate was compared to previous ones and differences were analyzed further. The temporal and spatial variations of the ^{137}Cs concentration present in the coastal waters were shown to be strongly related to the wind intensity and direction. During the first month after the accident, winds blowing toward the south confined the radionuclides directly released into the ocean to a narrow coastal band. Afterwards, frequent northward wind events increased the dispersion over the whole continental shelf, leading to strongly reduced concentrations.

Citation: Estournel, C., et al. (2012), Assessment of the amount of cesium-137 released into the Pacific Ocean after the Fukushima accident and analysis of its dispersion in Japanese coastal waters, *J. Geophys. Res.*, *117*, C11014, doi:10.1029/2012JC007933.

1. Introduction

[2] The accident at the Fukushima Daiichi nuclear power plant following the earthquake and the tsunami of 11 March 2011 released large amounts of radioactive material into the atmosphere, through explosions of the upper cladding of some reactor units, and also directly into the ocean at the power plant, through leakage, operations for reactor cooling and planned discharge of excess low-level radioactive water. Part of the release to the atmosphere was also transferred into the ocean through wet and dry deposition. The effect of these releases on the marine biota will doubtless be the subject of numerous studies, but a prerequisite for such studies is the determination of the total amount of isotopes released and the time-dependence of the release function (the source term), together with a definition of the areas affected by different levels of contamination and the duration of this contamination. The observations of ^{131}I and ^{137}Cs performed daily by TEPCO (Tokyo Electric Power Company, the power plant operator) and MEXT (Japanese Ministry of Education, Culture, Sports, Science and Technology) are invaluable for attempts to answer these questions but, clearly, numerical simulation is the tool that permits the gaps in the sampling to be filled and budgets to be calculated, provided the simulations are reasonably well validated by comparison with the available observations.

[3] As stressed by *Tsumune et al.* [2012], comparisons among models will be useful to improve our knowledge of these questions. For instance, they should enable the uncertainties on the source term to be assessed insofar as the various groups involved in the modeling task use different models with different numerical methods, different implementations (domain, mesh, forcing) and different approaches. This paper

[1]SIROCCO Group, Laboratoire d'Aérologie, Université de Toulouse, CNRS, Toulouse, France.
[2]Environment Laboratories, IAEA, Monaco.
[3]Joint Laboratory Ecole des Ponts ParisTech and EDF R&D, CEREA, Université Paris-Est, Champs-sur-Marne, France.
[4]INRIA, Paris Rocquencourt Research Centre, Paris, France.
[5]SIROCCO Group, LEGOS, Université de Toulouse, CNRS, Toulouse, France.

Corresponding author: C. Estournel, SIROCCO Group, Laboratoire d'Aérologie, Université de Toulouse, CNRS, 14 Avenue Edouard Belin, FR-31400 Toulouse CEDEX, France. (claude.estournel@aero.obs-mip.fr)

0148-0227/12/2012JC007933

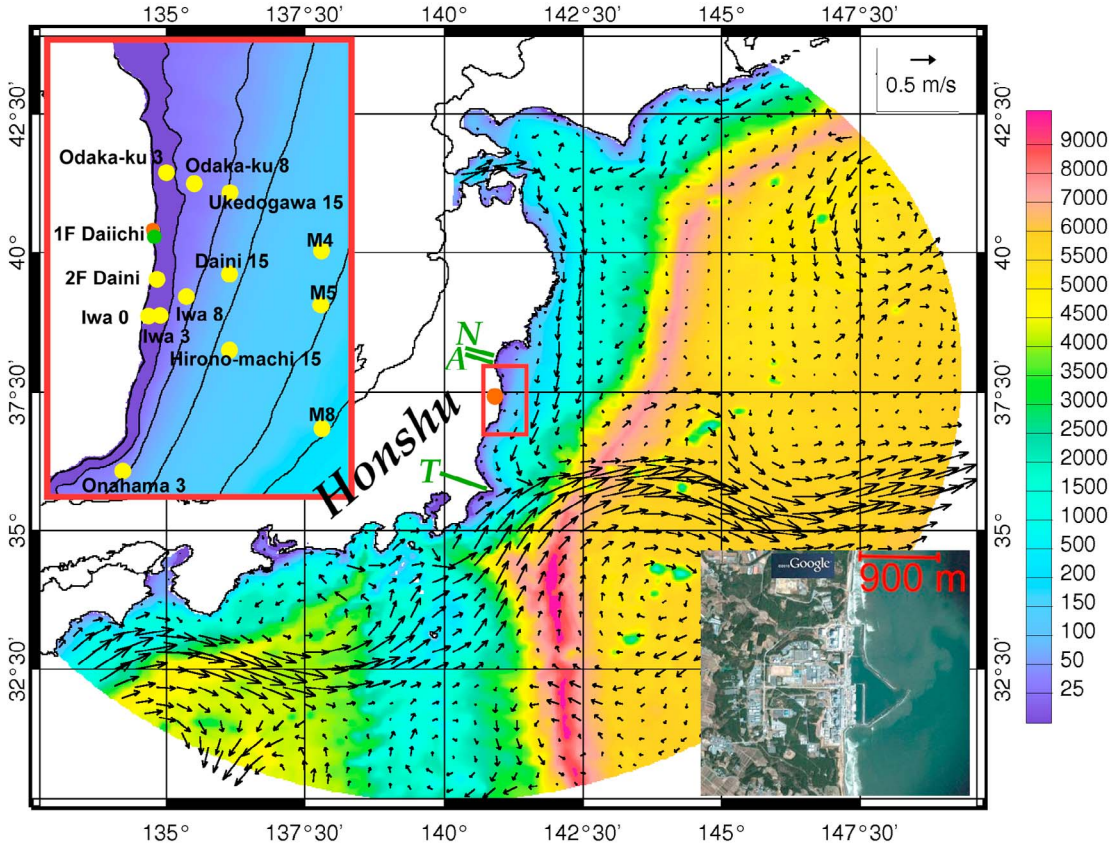

Figure 1. Numerical domain and its bathymetry. Surface current averaged over April is superimposed. The red circle indicates the position of the Fukushima Daiichi power plant. River mouths are indicated with green bars (N for Natori R., A for Abukuma R. and T for Tone R.). The red rectangle indicates the position of the top left inset giving the location of observation sites (section 5). Bottom right inset (plotted with Google Earth) displays the geometry of the power plant with its seawalls. The two outlets mentioned in the text are outside the seawalls to the north and south of the power plant.

is a contribution to this intercomparison. A numerical high-resolution simulation and an inverse method are employed to calculate the daily flux of ^{137}Cs released directly to the ocean, using concentrations measured at the northern and southern outlets of the power plant. The paper first presents the hydrodynamic context of the contrasting coastal and deep-sea regions surrounding Fukushima. After a description of the method, an estimate of the source term is given and compared to previous studies. The validation of the method through comparisons with observations taken at different locations around the power plant is then presented. The dispersion of radionuclides at different time scales, together with the processes responsible for it, is discussed.

2. Topographic and Hydrodynamic Context

[4] The Fukushima Daiichi NPP is located on the eastern coast of Honshu Island, the main island of Japan (Figure 1). The eastern coast of Honshu Island (north of 35°N) is characterized by a narrow continental shelf to the south, which widens in Sendai Bay to reach about 70 km. In front of the Fukushima Daiichi power plant, it extends 40 km offshore. The slope bounding the shelf goes down into the Japan Trench (~9000 m) and then rises to the abyssal plain at about 5000 m. The Fukushima Daiichi NPP is located in the Kuroshio-Oyashio Transition Area, which is the region of confluence of the two western wind-driven boundary currents (WBC) of the North Pacific: the Kuroshio, which is the WBC of the subtropical gyre transporting warm, saline waters along the south coast of Japan and then eastward, and the Oyashio, which is the WBC of the subarctic gyre transporting, cold, fresh water southward [*Yasuda*, 2003]. The convergence of the two currents is marked by the creation of several intense mesoscale eddies, such as Kuroshio warm-core and cold-core rings. Another characteristic of the region is the Tsugaru Warm Current, flowing from the Sea of Japan through the Tsugaru Strait [e.g., *Yasuda et al.*, 1988] and then southward along the slope of the east coast.

[5] Mesoscale structures interact with coastal waters when they impinge on the shelf break, creating cross isobath flow. This dynamics is able to affect the whole continental shelf where it is narrow (~10 km) or is limited to the external shelf where the continental shelf is wide. On the other hand, shallow shelf waters respond to the winds and barotropic/baroclinic pressure gradients (tides, density gradients induced by fresh-water inputs, etc.). Thus two regions with different physical processes have to be considered regarding the dispersion of the radionuclides released directly into the ocean. Before reaching

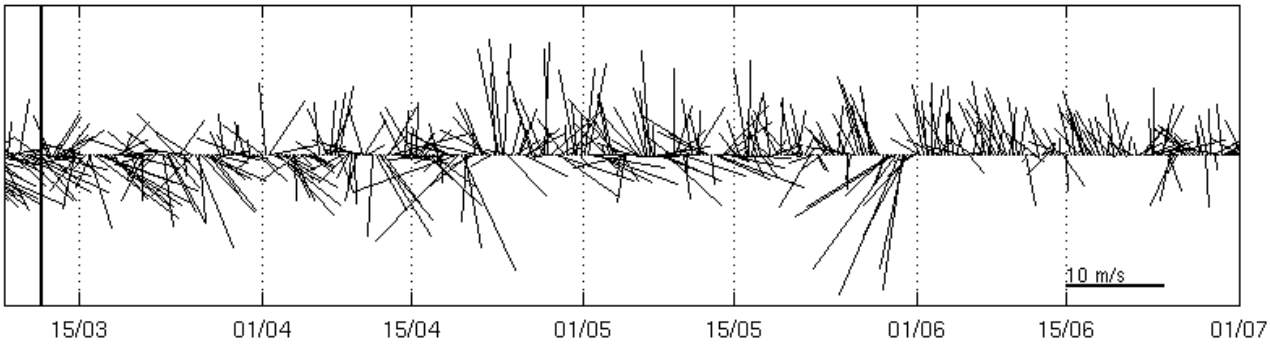

Figure 2. Time series of the ECMWF wind in the vicinity of the Fukushima power plant.

the open ocean, where large scale currents and mesoscale structures will transport and disperse them at basin scale, the radionuclides are transported by the coastal circulation on the continental shelf, where impacts on human activities and living resources can be expected to be the most significant. Let us now focus on the specificities of the latter region, which is central to this paper. The existence of a coast creates a blocking effect that reduces dispersion and induces dominant alongshore transport. During the three months following the accident, the strongest winds most often blew toward the south (southeast or southwest) and toward the north (Figure 2). In the first case, the wind induced downwelling, with surface waters pushed against the coast and the emergence of a coastal jet flowing southward. In the second case, the wind produced an upwelling. The alongshore component of the transport was northward but the Ekman drift tended to spread coastal waters toward the external shelf and the slope. This dispersal favored the interaction with the offshore currents flowing southward along the slope (Tsugaru and Oyashio Currents as well as the residual tidal current). The fallout of atmospheric radionuclides transported through the atmosphere impacted ocean surface beyond the continental shelf. Thus, some of these radionuclides possibly interacted with mesoscale structures characteristic of the region, which made their dispersion more efficient.

3. Material and Methods

[6] The method used to estimate the amount of ^{137}Cs released directly to the ocean relied on: (1) a 3D hydrodynamic model simulating the oceanic circulation over several months, (2) a model for the advection-diffusion of tracers based on currents and vertical diffusivities computed by (1), (3) an atmospheric dispersion model providing wet and dry deposition fluxes on the land and sea surface and (4) an inverse method calculating the direct release from the NPP day by day. The inverse method required the calculated daily average concentration of ^{137}Cs in the vicinity of the NPP to be as close as possible to the TEPCO measurements (usually 4 measurements per day, 2 to the north and 2 to the south of the plant). The four steps described above introduced uncertainties in the final result. Therefore, model results were compared to observations of ^{137}Cs concentration available at several points located near the shore and at 3, 8, 15 and 30 km offshore (TEPCO and MEXT observations). On the one hand, these comparisons provided a check that the estimate of the source term was consistent and allowed its uncertainties to be assessed and, on the other hand, they gave a better understanding of how dispersion proceeded and where the most affected areas were.

3.1. Hydrodynamic Modeling

[7] We used the SYMPHONIE model described in *Marsaleix et al.* [2009, 2012]. This model has been used extensively in Mediterranean coastal regions [*Estournel et al.*, 2005; *Ulses et al.*, 2008] and in the deep basin [*Herrmann et al.*, 2008]. The vertical grid is based on a generalized s-coordinate system. The 30 vertical levels were irregularly distributed, with increased resolution near the sea surface. The horizontal grid corresponded to the orthogonal curvilinear system used by *Michaud et al.* [2012] with the pole of the grid at 37.5°N, 140°E, corresponding to the center of the circle shown on Figure 1. The horizontal resolution was variable and increased linearly with the distance from the Fukushima NPP, where the size of the grid mesh was about 600 m. At the open lateral boundaries, the horizontal resolution reached its maximum value of 5.5 km. Figure 1 presents the numerical domain.

[8] The model was initialized and forced at its lateral boundaries with the global NCOM real-time operational ocean model of the U.S. Navy [*Barron et al.*, 2006] operated by NOAA and distributed through OceanNomads (http://www.northerngulfinstitute.org/edac/ocean_nomads.php). Temperature and salinity fields were restored to the large scale simulation with a nudging time scale of 1 month. Atmospheric forcing was computed from the ECMWF (European Centre for Medium-Range Weather Forecasts) model, which provided radiative fluxes and atmospheric parameters at a horizontal resolution of 1/4° and a temporal resolution of 3 h. These were used to calculate turbulent air sea fluxes according to the bulk formulae of *Estournel et al.* [2009]. Tides were computed with the finite element model T-UGO [*Pairaud et al.*, 2008], from which the components of the current and the sea surface elevation fields were extracted. These were introduced at the lateral open boundaries of the SYMPHONIE model using the boundary conditions described by *Marsaleix et al.* [2006]. Following *Pairaud et al.* [2008], the astronomical potential and a loading self attraction tide potential computed by T-UGO were taken into account in the SYMPHONIE momentum equations. The intensity of the residual tidal current that followed the coast southward, ranged from 1 to 2 cm/s in the region of the Daiichi NPP. The main rivers of the region (between 35.5 and 38.5°N), the Tone to the south, and the Natori and Abukuma to the north (Figure 1), were introduced into the model on the basis of

Table 1. Dry, Wet and Total Deposition of ^{137}Cs (in PBq) Over Different Regions Using Different Values for the Dry Deposition Velocity Over the Sea

	Dry Deposition Velocity		
over land	0.2 cm.s^{-1}	0.2 cm.s^{-1}	0.2 cm.s^{-1}
over sea	0.005 cm.s^{-1}	0.01 cm.s^{-1}	0.02 cm.s^{-1}
	Deposition Over North Pacific Ocean		
Dry deposition	0.1 PBq	0.3 PBq	0.5 PBq
Wet scavenging	5.6 PBq	5.6 PBq	5.4 PBq
Total	5.7 PBq	5.8 PBq	5.9 PBq
	Deposition Over North Pacific Ocean Within a Radius of 80 km		
Dry deposition	0.04 PBq	0.08 PBq	0.14 PBq
Wet scavenging	0.19 PBq	0.18 PBq	0.18 PBq
Total	0.23 PBq	0.26 PBq	0.33 PBq

climatological freshwater discharges (190, 17 and 67 m^{3}s^{-1} respectively), using the lateral momentum and salt boundary conditions of *Reffray et al.* [2004].

[9] The model was initialized on February 21st. Currents and vertical diffusivities computed by the model were averaged over 3-h periods and stored to compute the advection and diffusion of tracers in offline mode. This period was chosen as a compromise between the explicit representation of the tidal cycle and the amount of memory necessary to store the files. A sensitivity test to higher frequency storage (1 h) showed negligible differences.

3.2. Atmospheric Source

[10] The atmospheric ^{137}Cs source term was estimated using the Polyphemus/Polair3D transport model previously validated on radionuclide dispersion events (Algeciras, Chernobyl [see *Quélo et al.*, 2007]). Two simulation domains were used. The first covered Japan and also all of the North Pacific Ocean and a part of North America at a resolution of 0.25°. The atmospheric dispersion model was then driven by the ECMWF meteorological fields at a resolution of 0.25°. Another domain with a more refined mesh was used for the dispersion over Japan and near the Japanese coasts, at a resolution of 0.05°. For this simulation, meteorological fields at a resolution of 6 km were obtained by using the WRF (the Weather Research & Forecasting Model) model. This simulation gave more precise patterns for the radioactive material deposited over the coastal region, which was important in this study.

[11] The estimation of the total quantity of ^{137}Cs released into the atmosphere from the Fukushima-Daiichi NPP, together with the temporal profile of the release, were crucial to the atmospheric dispersion model that simulated deposition over the ocean. In this study, the atmospheric source term estimate from *Winiarek et al.* [2012] was used. This estimate was obtained by inverse modeling. For this purpose, a first guess was built up using the temporal profiles of the TEPCO gamma dose measurements taken at the Fukushima-Daiichi NPP site. This first guess was then taken as a background term in the inverse modeling algorithm using the available ^{137}Cs activity concentration data. In this specific study, the radioactive plume that yielded deposition over the North Pacific Ocean was the most important atmospheric pathway. It would have been unwise to use a release estimate obtained only by inverse modeling of activity concentrations in this case, because these observations were all located over land and the observability of the releases directed toward the ocean was not sufficient to constrain the release profile during these periods. In this situation, the gamma dose measurements gave the most valuable information about the releases and the plume moving toward the sea. The total estimated ^{137}Cs release from this source term was 17 PBq, which is of the same order of magnitude as that obtained by inverse modeling by *Chino et al.* [2011] for the Japanese Atomic Energy Agency: 13 PBq, and *Stohl et al.* [2012]: 37 PBq.

[12] The particles of ^{137}Cs were simply modeled as monodispersed. The wet scavenging was parameterized using a scheme based on a relative humidity threshold (see *Winiarek et al.* [2012] for details). The dry deposition was parameterized using a constant uniform velocity of v = 0.2 cm s^{-1} over the land, consistent with its estimation via data assimilation in the context of the Chernobyl accident [*Bocquet*, 2012], and a smaller constant uniform velocity over the sea. Following *Seinfeld and Pandis* [1998], this value was between 0.005 cm.s^{-1} and 0.02 cm.s^{-1}, depending on the size of the particles. We performed simulations using these two values to evaluate the sensitivity of the results to this parameterization (see Table 1). The additional value of 0.01 cm s^{-1} was taken as a median reference value, for which a simulation was also carried out. From the simulations, the results of which are reported in Table 1, we found a dry deposition between 0.1 PBq and 0.5 PBq over the Pacific Ocean and a total deposition between 5.7 PBq and 5.9 PBq (which is close to the Japanese Atomic Energy Agency estimation of 5.0 PBq). Within a radius of 80 km around the NPP, we found a dry deposition quantity between 0.04 PBq and 0.14 PBq (between 0.23 PBq and 0.33 PBq for the total deposition). The total ocean deposition was slightly sensitive to the dry deposition velocity near the coastal region but hardly sensitive at larger scale because wet scavenging was predominant and dry deposition velocity over the ocean became of lesser importance.

[13] For this study, we chose to use the deposited quantities and patterns from the median configuration simulation using v = 0.2 cm.s^{-1} over the land and v = 0.01 cm.s^{-1} over the sea. The map of total ^{137}Cs deposited on the sea surface with these dry deposition velocity values is displayed in Figure 3.

3.3. Direct Liquid Release

[14] The Fukushima Daiichi NPP is divided into two reactor groups. In front of the power plant, a set of seawalls protrudes into the ocean over a distance of about 700 m (see inset at bottom right of Figure 1), with the water intake in the middle and water discharge outlets outside the seawalls on either side. The distance between the two outlets located north and south of the power plant is about 1300 m. ^{137}Cs concentrations were generally measured twice a day, 30 m from the northern outlet and 300 m from the southern outlet. The 600 m mesh size of the model allowed us to represent this configuration schematically. The coastline was rectilinear around the power plant. The radionuclide flux was prescribed as a surface flux at the two grid points adjacent to the coastline corresponding to the two outlets. These two points were separated by 1200 m (two mesh steps, very close to the real distance of 1300 m), meaning that the only grid point between them corresponded to the port of the power plant inside the seawalls. This grid point was considered as a land

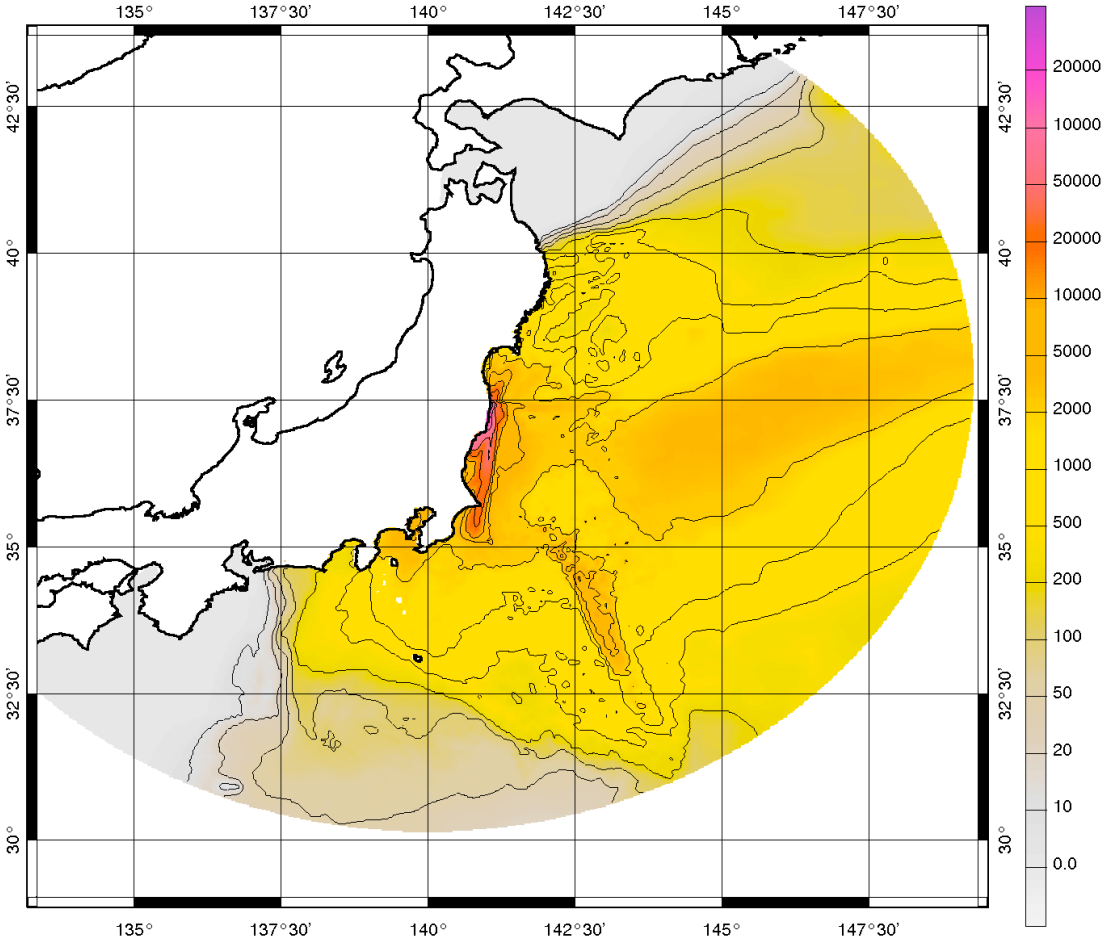

Figure 3. Total deposition of atmospheric ^{137}Cs (Bq/m^2) on the sea surface.

point in order to simulate the blocking effect of the seawalls. Such a simple grid geometry does not match the reality of the situation as radioactive leaks were detected inside the area delimited by the seawalls and not at the outlets. A correct representation of the geometry of the release area would have required a much finer grid than the one used here. Our grid was, nevertheless, a reasonable way of controlling the emission terms using the observations close to the two outlets.

[15] Radioactive decay was not taken into consideration as the physical half-life of ^{137}Cs (30 years) is much longer than the duration of our simulation. It was assumed that all the cesium was in dissolved form and thus did not interact with suspended matter. This hypothesis probably induced an overestimation of the simulated concentrations, especially since the suspended matter concentration may have been particularly high in the coastal zone due to the tsunami. Given that a Kd value of 4. 10^3 l/Kg [*International Atomic Energy Agency*, 2004] was taken to characterize the equilibrium partitioning of cesium between the dissolved and particulate phases in coastal environments, this effect could be expected to be low compared to other uncertainties (4% of cesium in particulate form for a suspended matter concentration of 10 mg/l).

[16] The inverse method to determine the source term was based on the following principle. The advection diffusion equation using an upwind scheme [*James*, 1996] was integrated 4 times a day. For the first run, a first guess was used for the value of the ^{137}Cs fluxes at the two input grid points (F_1 and F_2). The daily averaged concentrations of ^{137}Cs (C_1 and C_2) obtained after this run (sum of the contributions of the atmospheric source and direct release) was compared to the mean observed value at the same two points. In the second run, a variation of the input flux by a factor of 4 (reduction or increase depending on the result of the first run, the final result not being sensitive to this value) was imposed at the northern outlet while the flux at the southern outlet was kept unchanged. The third run was symmetrical to the second except that the southern outlet flux varied while the northern outlet flux was unchanged. The "true" fluxes at the two outlets were then calculated by solving a system of two linear equations with two unknowns expressing the variation of concentration at each source point (C_1 and C_2) as a function of the variation of the two input fluxes F_1 and F_2:

$$\Delta C_1 = \frac{\partial C_1}{\partial F_1}\Delta F_1 + \frac{\partial C_1}{\partial F_2}\Delta F_2$$

$$\Delta C_2 = \frac{\partial C_2}{\partial F_1}\Delta F_1 + \frac{\partial C_2}{\partial F_2}\Delta F_2$$

where $\frac{\partial C_1}{\partial F_1}$ and $\frac{\partial C_2}{\partial F_1}$ were calculated by combining Runs 1 and 2 and $\frac{\partial C_1}{\partial F_2}$ and $\frac{\partial C_2}{\partial F_2}$ by combining Runs 1 and 3. The quantities

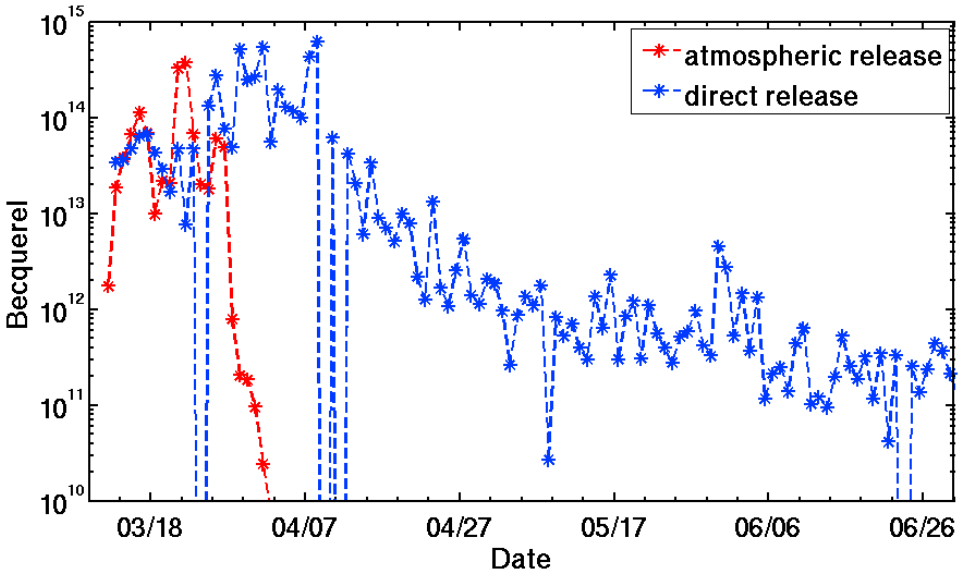

Figure 4. Daily ^{137}Cs release to the ocean (in Bq), red: coming from the atmosphere, blue: from the direct release and calculated by the inverse method.

ΔC_1 and ΔC_2 were calculated from the differences of concentration between the observations and Run 1 results. Solving the system allowed the two fluxes ($F_1 = \Delta F_1 - F_{1,run1}$ and $F_2 = \Delta F_2 - F_{2,run1}$) to be calculated. They were then injected into Run 4. It was checked that Run 4 provided concentrations very close to those observed (see the first two stations on Figure 5 below). Then the 4-step procedure was applied to the next day, starting from the archived results of Run 4 and from the calculated fluxes as first guess.

[17] No observations of the concentration were available before 21 March near the southern outlet or before 23 March near the northern outlet. In order to estimate the contribution of this period not covered by observations to the total release starting from 12 March, two simulations were carried out with different hypotheses. The first simulation assumed a constant concentration from 12 March to 21/23 March that was equal to the first observation available (1484 Bq/l at the southern outlet on 21 March and 1900 Bq/l at the northern outlet on 23 March). The second simulation was an extreme case for which zero release was assumed before the first observation. The first simulation cannot be considered as the opposite extreme (highest release) a priori but comparisons with data at distant sites (see section 5) allowed us to analyze how realistic it was. Another test was done to estimate the sensitivity of the inverse method to the atmospheric release. In this test, the atmospheric release term was removed, meaning that the inverse method calculated a release rate that, alone, had to reproduce the observed concentrations at the NPP. The objective of this test was to determine the method's sensitivity to the accuracy of the atmospheric deposition estimate.

4. Amount of ^{137}Cs Released Directly Into the Ocean

[18] Figure 4 presents the daily integrated activity of ^{137}Cs corresponding to the direct release to the ocean between 12 March and 30 April for the scenario assuming concentrations in seawater from 12 to 21/23 March equal to the first observation. The atmospheric deposition on the sea surface integrated over the whole modeling domain is also presented. Table 2 summarizes the cumulated release and allows a comparison with previously published estimates. It should be noted in passing that the release of ^{134}Cs can be expected to be similar to that of ^{137}Cs, based on the fact that the isotopic ratio in seawater is close to 1 [*Buesseler et al.*, 2012].

[19] The difference between our two scenarios for the no-observation period (4.1 PBq for a nil release and 4.5 PBq in the other case) indicates that, within the limit of our sensitivity test, the amount of ^{137}Cs released to the ocean before 21 March was only 8% of the total liquid release. Besides, 99% of the total ^{137}Cs released was discharged into the ocean before 22 April. Daily liquid releases of ^{137}Cs in May were 300 times lower than during the period of maximum release (end of March–beginning of April). During the maximum release period, the direct release varied by a factor of 10.

[20] The test without the atmospheric release showed very small differences with the reference case. This was because the direct liquid release was, on the whole, the dominant term in the close vicinity of the power plant. By analyzing the

Table 2. Amount of ^{137}Cs Released Into the Ocean[a]

Origin of the Estimate	^{137}Cs Activity Released to the Ocean (PBq)
TEPCO (1–6 April)	0.94
JAEA (21 March–30 April)	4
CRIEPI (26 March–31 May)	3.5 +/ −0.7
IRSN (26 March–8 April)	27
Inverse method of this study (12 March–30 June)	4.1–4.5
Inverse method of this study (1–6 April)	0.81

[a]Estimates by TEPCO and JAEA from *Kawamura et al.* [2011], estimate by CRIEPI from *Tsumune et al.* [2012], estimate by IRSN from *Bailly du Bois et al.* [2012].

$^{131}I/^{137}Cs$ ratio, *Tsumune et al.* [2012] found that 26 March marked a transition between a situation dominated by atmospheric deposition before that date and direct release after. So atmospheric deposition might significantly impact our inverse method only between 23 March (date of the beginning of the regular monitoring at the two outlets of the NPP) and 26 March. This is clearly not a period that represents the largest part of the total direct release.

[21] Our release estimate between 1 and 6 April was close to that of TEPCO, which was based on an estimate of the volume of outflow and the concentration of ^{137}Cs in the outflow water. On the other hand, strong releases calculated on 7 and 8 April in relation with high measured concentrations (68000 Bq/l on 7 April and 34000 and 29000 Bq/l on 8 April) could appear to be in contradiction with the fact that TEPCO injected sodium silicate on 6 April to stop the visible direct leak from the reactor 2. This may be illustrative of the delay introduced by the countermeasures and the seawall. As already mentioned, the leakage was in the port inside the seawalls and not at the outlets. The exchanges between the port and the open sea were complicated by the seawalls (partly broken after the earthquake). This means that our release rate cannot be considered as representative of the leakage from the NPP at the precise dates indicated in Figure 4 as the transfer from the port to the outlets could create a delay. Precise modeling of the NPP geometry would be necessary to elucidate this point, which is not central to our study.

[22] Over the whole period, our estimate is very close to the JAEA estimate, itself using the TEPCO estimate between 1 and 6 April to calibrate the transformation of concentration in front of the power plant into fluxes. Our estimate is also close to that of CRIEPI, which is based on a general principle close to ours except for the fact that they determined the time-average of the release rate for 26 March–6 April from the average of the concentration measured at the two sites while we determined the flux day by day from the daily concentration. Besides the close agreement of these different estimates, it is very interesting to observe that our inverse method gives a strong increase in direct release ($>10^{14}$ Bq/l) on 25 March (Figure 4). This result is in rather good agreement with *Tsumune et al.* [2012] who estimated the beginning of direct releases as 26 March. Finally, our estimate and the previous ones are 5 times lower than the estimate of IRSN, which used spatial interpolation of the whole set of observations available over 7-day time slices. This discrepancy will be discussed in Section 8.

[23] A way to estimate the accuracy of our inverse method is to assess its ability to simulate concentrations close to those observed by sampling in different locations around the power plant. These observations are particularly suited for the validation as they were not used in the inverse method.

5. Validation of the Method and Alongshore Dispersion of ^{137}Cs

[24] Observations of ^{137}Cs concentrations near the outlets of the power plant were used in the inverse method to calculate the amounts of radionuclides released after the accident. Systematic comparisons were made between the simulation results and all the observations available at remote sites to check that the fluxes deduced from the inverse method were consistent with the whole set of data. This consistency was necessary if the simulation was to be suitable for studying the dispersion. We selected several sites located in different directions (Figure 1). Two alongshore points were selected, off the Fukushima 2F Daini power plant, 11.5 km south of Daiichi, and off Iwasawa, 16 km south of Daiichi. They had been monitored basically every day since 21 March. Among the different monitored sites located 3 km offshore along a 80 km north-south coast segment, we chose three sites: one to the north named "3 km offshore of Odaka-ku" by TEPCO and located 14 km from Daiichi, one to the south, "3 km offshore of Onahama Port" at 58 km from Daiichi, and an intermediate one "3 km offshore of Iwasawa shore" 20 km from Daiichi. These three sites gave indications on the alongshore dispersion. Two sites were chosen at 8 km from the shore: the first "8 km offshore of Iwasawa shore" and the second one "8 km offshore of Odaka-ku." Three sites were chosen at 15 km offshore, from north to south: "15 km from the coast of Ukedogawa River," "15 km from the coast of Daini" and "15 km from the coast of Hirono Town." Three MEXT sites located 30 km from the shore were chosen: M4, M5 and M8. M4 and M5 were the two MEXT sites where the largest concentrations were observed. Figure 5 presents comparisons at the 13 sites, each site being named by its short name followed by its distance from the shore. The observations at the two outlets of Daiichi are also shown, to evaluate the orders of magnitude of the dilution. Vertical dashed bars stand for observations below the detection limit, itself indicated by the red dashed line. (Note that the value of 15 Bq/L is only indicative for TEPCO stations. As TEPCO explained, the value depended on detectors and samples, as attested by values lower than this threshold. 10 Bq/L is displayed for MEXT sites, as given in the MEXT reports.) Results of both simulations, with and without input during the initial phase, are presented on the 2F Daini NPP site.

[25] During the period of strong inputs (between 25 March and 8 April), the confinement of radionuclides near the NPP was significant, the concentration measured there being about 20 times higher than at 11 km to the south (2F Daini 0 km) which, after the NPP, is the monitored site where measured concentrations were the highest. Simulated concentrations were well validated at this site. The simulation based on constant concentration at the power plant during the no-observation period being equal to the first observation produced overestimated concentrations at 2F Daini 0 km during this phase, while the extreme case with a nil concentration during this period was rather underestimated. This means that the direct release was between these two cases, at least at the end of this period. Another sensitivity test with a high concentration of $^{137}Cesium$ imposed only from 12 to 15 March, showed that the first observations at Daini 0 km were available too late to capture these hypothetical early events. Thus, the release during the first days after the accident cannot be estimated from the available observations.

[26] A careful analysis of the curves indicated drops in the concentration at the NPP on 26 March (Daiichi South) and 2 April (Daiichi North), which were shortly followed by increases at 2F Daini. This southward advection of the contamination is likely due to the occurrence of two moderate southeastward wind gusts (10 m/s). At the same time, the inverse method calculated a decrease in the direct release. In a general way, it is difficult to assess the validity of such rapid variations of the direct release. A poor representation

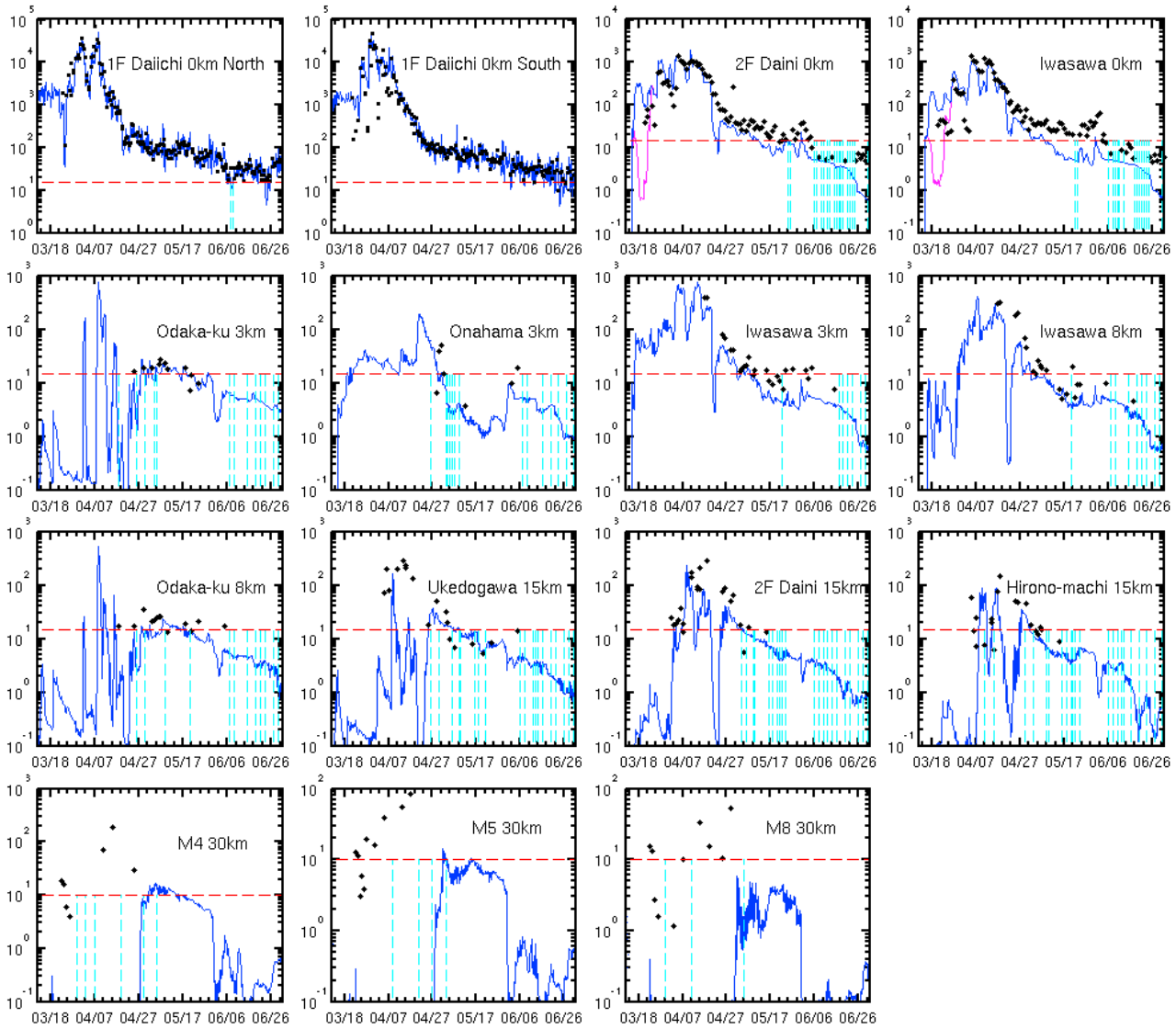

Figure 5. Comparison of ^{137}Cs concentrations observed (asterisk) and simulated (solid line) at different points indicated in the frames (the name of the stations is followed by the distance to the coast). See map on Figure 1 for precise locations. The red dashed line indicates the detection limit while vertical cyan dashed lines indicate observations below the detection limit. The blue line corresponds to the simulation with concentration during the no-observation period set equal to the first observation available, the magenta line (only shown at 2F Daini 0 km and Iwasawa 0 km) is for nil concentration during this period.

of advection processes could be counterbalanced by artificial variations in the release. For instance, for wind conditions favorable to offshore dispersion of radionuclides, an underestimation of the wind in the model could induce too strong a confinement of radionuclides at the NPP and the inverse method would then compensate by a decrease of the release.

[27] In the cross shore direction, the sudden increases at 2F Daini were also detected at 3 km offshore (Iwasawa 3 km). At 8 km offshore (Iwasawa 8 km), the low-frequency dynamics of the concentration was close to the previous ones but rapid variations observed near the coast did not always exist there. North and south of the domain, the simulation reproduced the observations (unfortunately not numerous) quite well. The rapid variations simulated to the north (Odaka-ku 3 km) in April were also induced by wind gusts. For example, the occurrence of concentrations close to 1000 Bq/l on 8 April was associated with a strong decrease of concentrations at the NPP because of a moderate wind (8 m/s) blowing toward the northeast. The concentration simulated at the remote site of Onahama 3 km to the south did not exceed 100 Bq/l, except on 21 April, when all the sites located farther north recorded a marked decrease in the concentration, evidencing a southward advection of the contaminated water pool. Between 7 and 15 April, concentrations observed at 15 km offshore displayed values of about 100 Bq/l. The model simulated this order of magnitude even though an underestimation can be noted to the north (Ukedogawa 15 km). Nevertheless, the underestimation was very clear at stations located 30 km offshore as

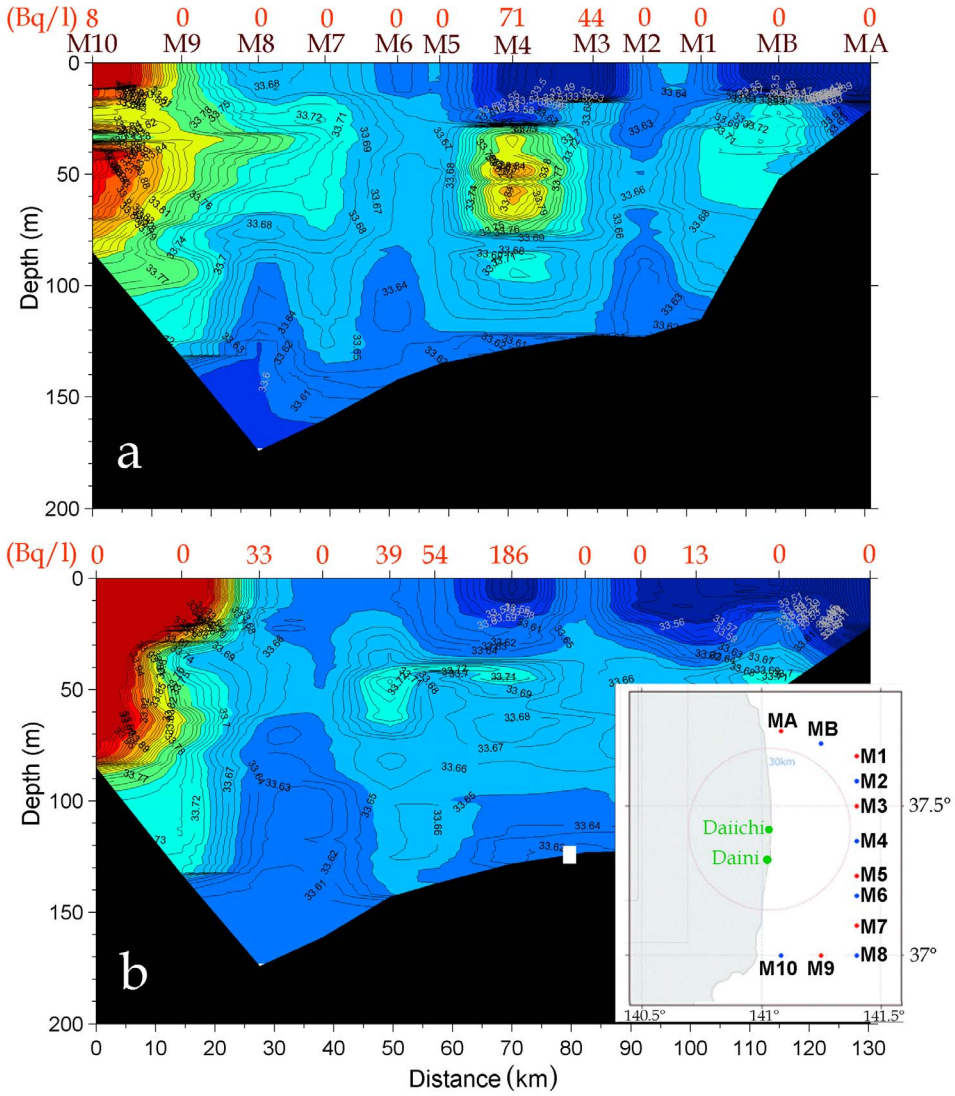

Figure 6. Vertical sections of salinity extracted from the JAMSTEC website: http://www.godac.jamstec.go.jp/monitoringdata/ for (a) April 9–11 and (b) April 13–15. The position of MEXT stations reported at the top of the figure is indicated in the inset extracted from the same website and slightly modified. ^{137}Cs concentration measured in the surface water at each station is reported in red above each station.

discussed by *Tsumune et al.* [2012] from the results of their model (their Figure 13). At 30 km, until 7 April, a background from atmospheric deposition existed (around 10 Bq/l) as inferred by *Tsumune et al.* [2012] from the ^{131}I/^{137}Cs activity ratio. This background could be underestimated by the atmospheric model but, clearly, it is not enough to explain the values above 40 Bq/l from 9 to 24 April.

[28] The conclusion is that, at least during March–April, in a region of about 50 km on either side of the NPP, radionuclides were predominantly transported in a narrow coastal band because wind gusts produced alongshore currents responsible for radionuclide advection. If we compare the sites of Odaka-ku 3 km and Iwasawa 3 km located at approximately the same distance from the plant, to the north and south respectively, it appears that, during the period of highest concentrations, the region south of the NPP was impacted for a longer period than the northern one. Cross-shore dispersion was also effective but more limited. The model underestimation of concentrations at 30 km could indicate an underestimation of the amount of ^{137}Cs released by the NPP. In the next section, the reasons for the concentrations being underestimated at 30 km and the consequences of this underestimation on the total release estimate are investigated.

6. Cross-Shore Dispersion of ^{137}Cs

[29] The Japan Agency for Marine-Earth Science and Technology (JAMSTEC) carried out oceanographic observations under the "Sea Area Monitoring Action Plan" (http://www.godac.jamstec.go.jp/monitoringdata/) of the Ministry of Education, Culture, Sports, Science and Technology (MEXT). Regular CTD profiles were measured at the MEXT stations, including the stations already presented at 30 km. CTD profiles (available on the Website given above) were obtained

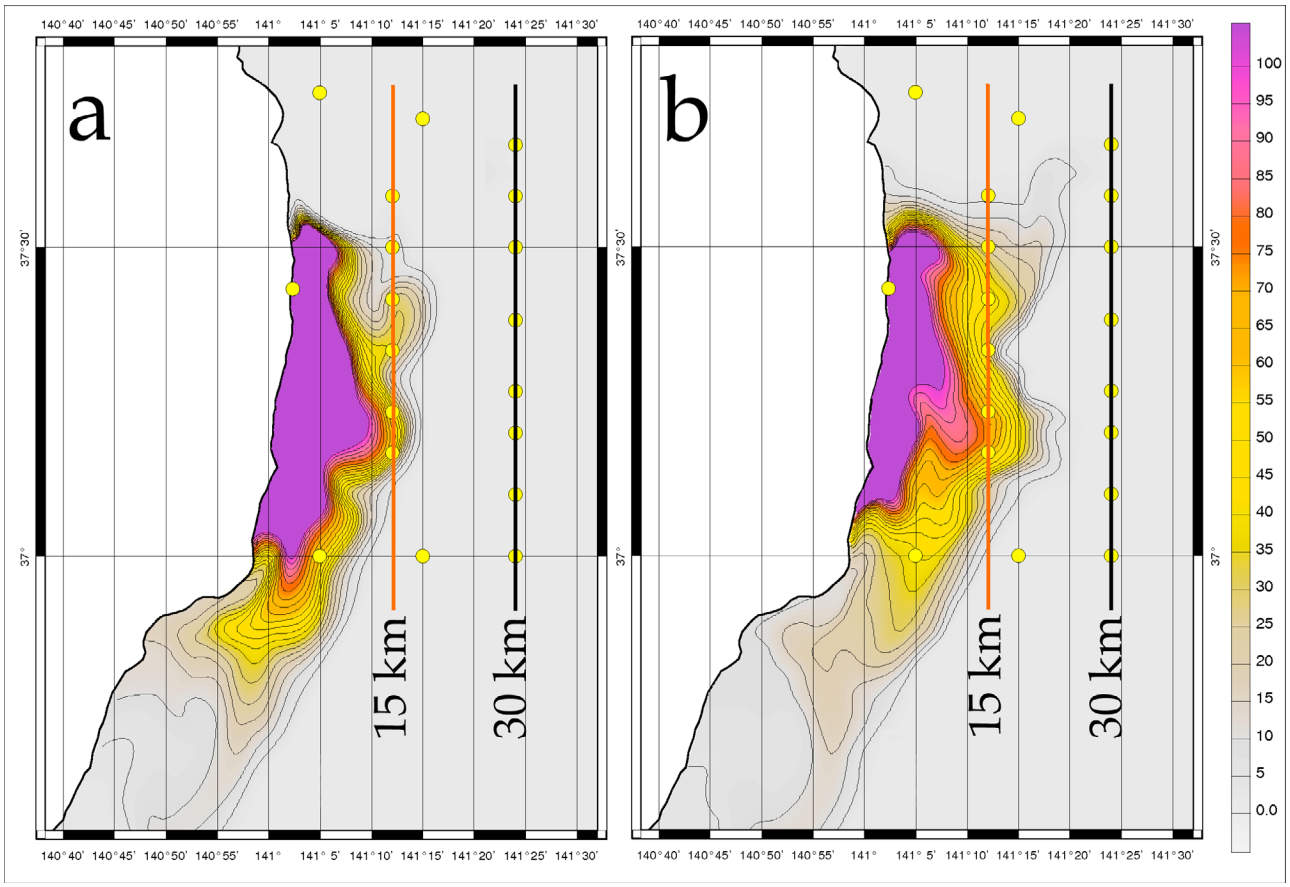

Figure 7. ^{137}Cs concentration at the ocean surface simulated for 15 April 2011. (a) reference simulation and (b) simulation with increased river discharges. The two lines join the stations located at 15 and 30 km offshore.

simultaneously with the measurement of ^{137}Cs concentration. Figure 6 presents two sections of salinity (figures downloaded from the JAMSTEC website) taken around mid-April when ^{137}Cs concentrations were the highest. These sections are the combination of CTD profiles obtained at two days of interval. Above each station, the number of the station, the date of sampling and the ^{137}Cs concentration has been added. The highest concentrations were associated with low salinity values located in the middle of the section and restricted to a surface layer. Low salinities were also present farther north but were little contaminated if at all. For each section, salinity profiles presenting the highest concentrations were examined. All these profiles presented a surface layer mixed over about 10 m, except station M5 on 13 April, for which the mixed layer depth was 20 m. It was then deduced that radionuclides were associated with a plume of coastal water influenced by river inputs, which was advected offshore, probably by wind action (more precisely the northward wind blowing episodically from 1 April and in particular between 6 and 8 April; see Figure 2). This thin freshwater layer was not present in our simulation. A test of sensitivity to the river discharges was done by multiplying them by a factor 5. Figure 7 presents the contours of the contaminated plume for the reference simulation and for the test. The river discharge increase produced a plume extending farther offshore and farther to the north. The underestimation at Ukedogawa 15 km was clearly reduced (not shown). Concentrations simulated at 30 km were still too low and concentrations were also too low alongshore to the south of the NPP (Daini 0 km and Iwasawa 0 km). Another uncertain hypothesis is that the river-influenced waters might originate from one of the numerous small rivers discharging in the region of the NPP (about 30 river mouths have been counted over a distance of 100 km).

[30] To conclude, observed cross-shore transport of radionuclides is related to the presence of fresh water in the region of the NPP. This fresh water is efficiently driven by the wind as the vertical salinity gradient reduces the exchanges with the denser underlying waters (the depth of this surface layer is only 10 m at 30 km from the NPP). The numerical simulation provides an approach to this situation but does not reproduce it faithfully, probably because the complexity of the spatial and time distributions of the river discharges were not accurately taken into account in our model. The ^{137}Cs inventory missing in the simulation was estimated by using the spatial interpolation of observations 15 km offshore between 11 and 18 April carried out by *Bailly du Bois et al.* [2012] (first panel of their Figure 4). Assuming that ^{137}Cs is present in a 15 m surface layer (overestimation of the low-salinity surface layer), a maximum value of 1 PBq is found by manual integration. This number added to the previous estimate of the total release by the inverse method provides an upper bound to our estimate of 5.5 PBq.

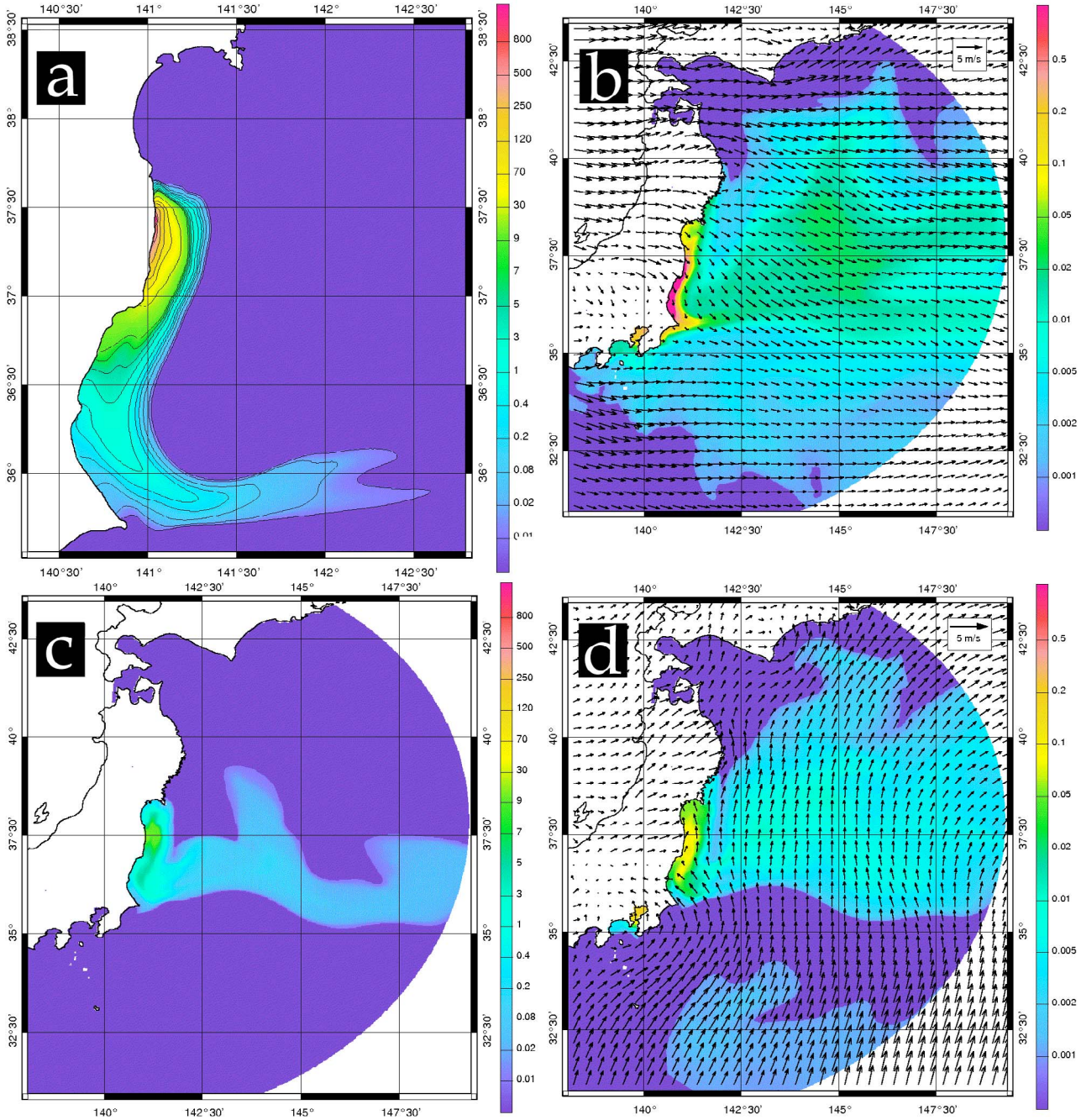

Figure 8. Mean ^{137}Cs concentrations (in Bq/l) near the surface over two periods of one month duration. (a and b) March 20–April 19 and (c and d) May. (left) Radionuclides from direct release and (right) atmospheric release. The mean wind field is superimposed in the right panel. Note the zoom in Figure 8a to show the confinement along the coastline during the first month and the different color bars for direct and atmospheric releases.

7. Dispersion of ^{137}Cs in the Coastal Region on the Monthly Scale

[31] At the end of June, ^{137}Cs concentrations were below 10 Bq/l at all observation sites except in front of the power plant. We have seen that, during the high input period (up to 8 April), radionuclides were strongly confined in the vicinity of the power plant. It was also shown that, in April, the occurrences of peaks of concentrations along the coast were caused by moderate wind increases, southward wind events inducing concentration increases at sites located south of the NPP and vice versa for northward winds. The objective of this section is to understand the characteristics of the dispersion during the period of strong decrease of contaminants in the coastal zone. Concentrations were averaged over two periods of one month (20 March–19 April and the

whole month of May). Figure 8 presents the mean concentration of ^{137}Cs (direct liquid release and atmospheric deposit) in the surface water during these two periods. The strong confinement discussed above is clearly visible during the first month after the accident, especially for the radionuclides directly released into the ocean (Figure 8a): spatial gradients are very sharp and the extent of impacted areas (considered arbitrary when concentration is higher than 1 Bq/l) is of the order of 3000 km^2. Note that the shape of the contaminated water pool along the Ibaraki coast (~36.5°N) could be biased as satellite images of the sea surface temperature indicated the presence of a weak warm core eddy-like feature that was not present in our simulation. This structure might have caused a separation of the contaminated plume from the coast more to the north than shown in Figure 8a. Concentrations of radionuclides from the atmosphere are much lower but, as expected, also more dispersed (Figure 8b). The situation evolves strongly in May (and the following months). The concentration maxima near the NPP are much lower (partly because strong emissions were over) but the impacted areas are also much larger (by a factor of 4 to 5), suggesting an increased dispersion, especially northward and eastward (Figure 8c). Wind regimes explain this general behavior (Figures 2, 8b, and 8d). During the first period, most of the wind events were southward, promoting a downwelling characterized by confinement along the coast. After 20 April, except for an exceptional event at the end of May, most of the wind events were northward, promoting an upwelling characterized by eastward spreading. Far offshore, concentration of ^{137}Cs deposited from the atmosphere decreased slowly (Figures 8b and 8d). Around 146°E at the end of April, its order of magnitude (0.01 Bq/l) was close to the observations reported by *Honda et al.* [2012] (0.06 Bq/l). Nevertheless, values are strongly underestimated in mid April around 143°E, apparently due to an over-powerful Oyashio current advecting "clean waters" into this region.

8. Discussion and Conclusion

[32] The originality of the method developed in this paper to calculate the source term relies on a simulation of the region around the power plant at a relatively high resolution, which makes for a realistic comparison of observed and simulated concentrations in the vicinity of the two outlets of the NPP. Also, the daily ^{137}Cs release is calculated to optimally adjust the mean concentration deduced from the two daily observations at the two points. The good agreement of the simulation with the coastal observations and the adjustment of the concentrations at the power plant demonstrate the validity of our specification of the source term. A bias of the model is, however, noticed at 30 km offshore. This bias results in an underestimate of the total ^{137}Cs release by 1 PBq, giving an upper value of the release estimate of 5.5 PBq. This value has the same order of magnitude as that of JAEA and CRIEPI. The source term estimated by *Bailly du Bois et al.* [2012], based on an analysis of observations, is much higher. We think that uncertainties on the two steps of their calculation could explain this large estimate. The first step is based on the estimate of the total inventory of ^{137}Cs in a box around the power plant through spatial interpolation of the data available, leading to a value of 11.6 PBq for 14 April (see their Figure 4a). This estimate could be biased, particularly north of the power plant, due to a lack of observations. In addition, in this region, the interpolation is strongly constrained by an observation taken on 17 April at Iwasawa 8 km (to the southeast of the power plant) (TEPCO, 2011, available at http://www.tepco.co.jp/en/press/corp-com/release/betu11_e/images/110418e12.pdf) misplaced to the northeast (at Odaka-ku 8 km). The second step of their estimate is the backward-in-time extrapolation (based on a constant dilution rate) of the inventory of 14 April, leading to its doubling on 8 April. In our modeling results, the inventory in the region discussed here is remarkably constant over this period (decrease of 7%) due to moderate wind conditions. The use of a dilution law deduced by *Bailly du Bois et al.* [2012] from observations running from April to July could introduce considerable uncertainty in their short-term extrapolation, which should be assessed with different approaches.

[33] Numerical modeling allowed an analysis of the dilution processes associated with the release of contaminants at the coastline. Contaminants coming from the Daiichi power plant stayed strongly confined along the coast for a relatively long time, mainly transported by the coastal wind-induced currents without being influenced by the intense mesoscale and large scale currents of the deep sea. Dispersion in the coastal zone was not isotropic. The presence of the coast favored the alongshore dispersion. However, two asymmetric cases have to be distinguished: when the wind blows southward as during the period of high input (mid March–mid April), the confinement at the coast is strong because of the Ekman drift directed toward the coast in such downwelling conditions. In contrast, the dominant northward wind blowing after mid April dispersed the radionuclides over the whole shelf because the Ekman drift was directed seaward, leading to strongly reduced concentration even if the total stock in the region did not decrease very markedly. Such a cross-shore dispersion event was detected around mid-April in the observations at 30 km but models underestimated it. Observations indicate that the presence of radionuclides offshore was associated with a thin, low-salinity surface layer. The presence near the NPP of freshwater discharged by rivers should have facilitated the offshore transport of radionuclides through the decoupling of the light surface layer from the denser underlying waters. The absence of information on the discharge of rivers makes the situation difficult to simulate with the numerical models.

[34] An important question concerns the possibility of transposing the conceptual model of dispersion learnt from the Fukushima accident to other regions. In a first (simplified) approach, the dispersion in the Fukushima Daiichi region could be representative of coastal regions bounded by wide continental shelves where the wind plays an important role. A very different case corresponds to coastal sites directly bounded by a steep slope. It can be expected that, in such cases, mesoscale turbulence and large scale circulation should disperse the contaminants more rapidly.

[35] The accident of Fukushima has demonstrated that numerical modeling coupled with observations of contaminant at the release point is a powerful tool to give early information about the extension of the contamination and its intensity. We would like to emphasize the importance of rapid access to observations by a wide and independent scientific community (as was the case after the Fukushima accident for radionuclide concentrations in the sea). Free and

open distribution of products such as accurate topography and operational atmospheric and oceanic forcing is also clearly an issue for a rapid response of the scientific community to emergency situations.

[36] **Acknowledgments.** The authors are most grateful to Frank Bub of the Naval Oceanographic Office for providing the NCOM files so promptly and kindly. They also warmly thank the members of the IT department of the Laboratoire d'Aérologie of CNRS and Toulouse University for their continuous support. The International Atomic Energy Agency is grateful to the Government of the Principality of Monaco for the support provided to its Environment Laboratories. This work was performed using HPC resources from CALMIP (grant 2011-P09115) and CINES.

References

Bailly du Bois, P., P. Laguionie, D. Boust, I. Korsakissok, D. Didier, and B. Fiévet (2012), Estimation of marine source-term following Fukushima Dai-ichi accident, *J. Environ. Radioact.*, *114*, 2–9, doi:10.1016/j.jenvrad.2011.11.015.

Barron, C. N., A. Birol Kara, P. J. Martin, R. C. Rhodes, and L. F. Smedstad (2006), Formulation, implementation and examination of vertical coordinate choices in the Global Navy Coastal Ocean Model (NCOM), *Ocean Modell.*, *11*(3–4), 347–375, doi:10.1016/j.ocemod.2005.01.004.

Bocquet, M. (2012), Parameter field estimation for atmospheric dispersion: Application to the Chernobyl accident using 4D-Var, *Q. J. R. Meteorol. Soc.*, *138*, 664–681, doi:10.1002/qj.961.

Buesseler, K. O., et al. (2012), Fukushima-derived radionuclides in the ocean and biota off Japan, *Proc. Natl. Acad. Sci. U. S. A.*, *109*, 5984–5988, doi:10.1073/pnas.1120794109.

Chino, M., H. Nakayama, H. Nagai, H. Terada, G. Katata, and H. Yamazawa (2011), Preliminary estimation of release amount of ^{131}I and ^{137}Cs accidentally discharged from the Fukushima Daiichi nuclear power plant into the atmosphere, *J. Nucl. Sci. Technol.*, *48*, 1129–1134, doi:10.1080/18811248.2011.9711799.

Estournel, C., V. Zervakis, P. Marsaleix, A. Papadopoulos, F. Auclair, L. Perivoliotis, and E. Tragou (2005), Dense water formation and cascading in the Gulf of Thermaikos (North Aegean) from observations and modelling, *Cont. Shelf Res.*, *25*, 2366–2386, doi:10.1016/j.csr.2005.08.014.

Estournel, C., F. Auclair, M. Lux, C. Nguyen, and P. Marsaleix (2009), "Scale oriented" embedded modeling of the north-western Mediterranean in the frame of MFSTEP, *Ocean Sci.*, *5*, 73–90, doi:10.5194/os-5-73-2009.

Herrmann, M. J., S. Somot, F. Sevault, C. Estournel, and M. Deque (2008), Modeling the deep convection in the northwestern Mediterranean Sea using an eddy-permitting and an eddy-resolving model: Case study of winter 1986–1987, *J. Geophys. Res.*, *113*, C04011, doi:10.1029/2006JC003991.

Honda, M. C., T. Aono, M. Aoyama, Y. Hamajima, H. Kawakami, M. Kitamura, Y. Masumoto, Y. Miyazawa, M. Takigawa, and T. Saino (2012), Dispersion of artificial caesium −134 and −137 in the western North Pacific one month after the Fukushima accident, *Geochem. J.*, *46*, e1–e9.

International Atomic Energy Agency (2004), Sediment distribution coefficients and concentration factors for biota in the marine environment, *Tech. Rep. Ser. 422*, 103 pp., Vienna.

James, I. D. (1996), Advection schemes for shelf sea models, *J. Mar. Syst.*, *8*, 237–254, doi:10.1016/0924-7963(96)00008-5.

Kawamura, H., T. Kobayashi, A. Furuno, T. In, Y. Ishikawa, T. Nakayama, S. Shima, and T. Awaji (2011), Preliminary numerical experiments on oceanic dispersion of ^{131}I and ^{137}Cs discharged into the ocean because of the Fukushima Daiichi nuclear power plant disaster, *J. Nucl. Sci. Technol.*, *48*(11), 1349–1356, doi:10.1080/18811248.2011.9711826.

Marsaleix, P., F. Auclair, and C. Estournel (2006), Considerations on open boundary conditions for regional and coastal ocean models, *J. Atmos. Oceanic Technol.*, *23*, 1604–1613, doi:10.1175/JTECH1930.1.

Marsaleix, P., F. Auclair, and C. Estournel (2009), Low-order pressure gradient schemes in sigma coordinate models: The seamount test revisited, *Ocean Modell.*, *30*, 169–177, doi:10.1016/j.ocemod.2009.06.011.

Marsaleix, P., F. Auclair, C. Estournel, C. Nguyen, and C. Ulses (2012), Alternatives to the Robert-Asselin filter, *Ocean Modell.*, *41*, 53–66, doi:10.1016/j.ocemod.2011.11.002.

Michaud, H., P. Marsaleix, Y. Leredde, C. Estournel, F. Bourrin, F. Lyard, C. Mayet, and F. Ardhuin (2012), Three-dimensional modelling of wave-induced current from the surf zone to the inner shelf, *Ocean Sci.*, *8*, 657–681, doi:10.5194/os-8-657-2012.

Pairaud, I. L., F. Lyard, F. Auclair, T. Letellier, and P. Marsaleix (2008), Dynamics of the semi-diurnal and quarter-diurnal internal tides in the Bay of Biscay. Part 1: Barotropic tides, *Cont. Shelf Res.*, *28*, 1294–1315, doi:10.1016/j.csr.2008.03.004.

Quélo, D., M. Krysta, M. Bocquet, O. Isnard, Y. Minier, and B. Sportisse (2007), Validation of the Polyphemus platform on the ETEX, Chernobyl and Algeciras cases, *Atmos. Environ.*, *41*, 5300–5315, doi:10.1016/j.atmosenv.2007.02.035.

Reffray, G., P. Fraunié, and P. Marsaleix (2004), Secondary flows induced by wind forcing in the Rhône region of freshwater influence, *Ocean Dyn.*, *54*, 179–196, doi:10.1007/s10236-003-0079-y.

Seinfeld, J. H., and S. N. Pandis (1998), *Atmospheric Chemistry and Physics: From Air Pollution to Climate Change*, John Wiley, New York, doi:10.1063/1.882420.

Stohl, A., P. Seibert, G. Wotawa, D. Arnold, J. F. Burkhart, S. Eckhardt, C. Tapia, A. Vargas, and T. J. Yasunari (2012), Xenon-133 and caesium-137 releases into the atmosphere from the Fukushima Dai-ichi nuclear power plant: Determination of the source term, atmospheric dispersion, and deposition, *Atmos. Chem. Phys.*, *12*, 2313–2343, doi:10.5194/acp-12-2313-2012.

Tsumune, D., T. Tsubono, M. Aoyama, and K. Hirose (2012), Distribution of oceanic ^{137}Cs from the Fukushima Daiichi Nuclear Power Plant simulated numerically by a regional ocean model, *J. Environ. Radioact.*, *111*, 100–108, doi:10.1016/j.jenvrad.2011.10.007.

Ulses, C., C. Estournel, P. Puig, X. Durrieu de Madron, and P. Marsaleix (2008), Dense shelf water cascading in the northwestern Mediterranean during the cold winter 2005: Quantification of the export through the Gulf of Lion and the Catalan margin, *Geophys. Res. Lett.*, *35*, L07610, doi:10.1029/2008GL033257.

Winiarek, V., M. Bocquet, O. Saunier, and A. Mathieu (2012), Estimation of errors in the inverse modeling of accidental release of atmospheric pollutant: Application to the reconstruction of the cesium-137 and iodine-131 source terms from the Fukushima Daiichi power plant, *J. Geophys. Res.*, *117*, D05122, doi:10.1029/2011JD016932.

Yasuda, I. (2003), Hydrographic structure and variability in the Kuroshio-Oyashio transition area, *J. Oceanogr.*, *59*, 389–402, doi:10.1023/A:1025580313836.

Yasuda, I., K. Okuda, M. Hirai, Y. Ogawa, K. Mizuno, and H. Kudoh (1988), Short-term variations of the Tsugaru Warm Current in autumn, *Bull. Tohoku Reg. Fish. Res. Lab.*, *50*, 153–191.